Electrochemical oxidation of carbon at high temperature: Principles and applications

Jiang Liu[1], Mingyang Zhou[1], Yapeng Zhang[1], Peipei Liu[1], Zhijun Liu[1], Yongmin Xie[1,2], Weizi Cai[1,3], Fangyong Yu[1,4], Qian Zhou[1], Xiaoqiang Wang[1], Meng Ni[3], and Meilin Liu[1,5]*

[1] Guangzhou Key Laboratory for Surface Chemistry of Energy Materials, New Energy Research Institute, School of Environment and Energy, South China University of Technology, Guangzhou 510006, P. R. China

[2] School of Metallurgy and Chemical Engineering, Jiangxi University of Science and Technology, Ganzhou 341000, Jiangxi Province, P. R. China

[3] Building Energy Research Group, Department of Building and Real Estate, The Hong Kong Polytechnic University, Hung Hom, Kowloon, Hong Kong, China

[4] School of Chemical Engineering, Shandong University of Technology, Zibo 255049, P. R. China

[5] School of Materials Science & Engineering, Georgia Institute of Technology, Atlanta, GA30332-0245, USA

ABSTRACT: Carbon is an important energy carrier. It is abundant in the world, richly existing in coal and biomass. Its energy is released mainly through oxidation. A heat energy of ~393 kJ may be obtained from the complete oxidation of 1 mol of carbon.

The most conventional way of carbon oxidation is combustion which has the problems of pollutant emission and low efficiency. However, through electrochemical oxidation, the chemical energy of carbon can be converted into electricity with high efficiency and low pollution. Herein, we give a brief review of our work on a novel technology of generating electricity and carbon monoxide from electrochemical oxidation of carbon, through a solid oxide fuel cell (SOFC) at high temperature. This so-called direct carbon SOFC (DC-SOFC) is with an all-solid-state configuration, without any purging gas or liquid medium. Electricity is generated by coupling of the electrochemical oxidation of CO at the anode and the reverse Boudouard reaction at the carbon fuel. Meanwhile, gaseous CO and CO_2 are produced. We prepared electrolyte-supported and anode-supported SOFC single cells and stacks and operated them directly with Fe-loaded activated carbon, biochar derived from orchid leaf and corn cob, respectively, as the fuel. Especially, we investigated their potential applications in portable power supplies and electricity-gas cogeneration. Our experimental results show that, the output performance of a DC-SOFC is comparable to that of a SOFC operated on hydrogen. A 3-cell-stack of tubular anode-supported segmented-in-series DC-SOFC gives a peak areal power density of 465 mW cm^{-2} and a volumetric power density of 710 mW cm^{-3}, at 850°C. Furthermore, the composition of the gas emission can be controlled by tuning the operating electrical current and the catalysts applied for the Boudouard reaction, so that CO gas and electricity co-generation can be realized.

1. INTRODUCTION

Generally, we define a matter containing carbon or/and hydrogen that can be automatically oxidized by oxygen to produce large amount of heat as a fuel. As an important energy element, carbon is richly reserved in fossil fuels and biomasses. Electricity is the most favored form of energy for terminal customers because it is convenient to use. Therefore, converting the chemical energy of carbon to electricity with high efficiency has always been important to human society. Conventional way of generating electricity from carbon is through internal combustion engine whose conversion efficiency is limited by Carnot efficiency. Meanwhile, pollutants such as NO_x may be emitted during the combustion process because air, with over 70% nitrogen, is directly fed into the engine. Low conversion efficiency results in more CO_2 production and emission, exacerbating the global climate change problem.

A fuel cell is an electrochemical device that can directly convert the chemical energy of a fuel to electricity through electrochemical reactions.[1,2] Its conversion efficiency is high because it is not limited by Carnot efficiency. In principle, any fuels can be oxidized electrochemically to generate electricity if oxygen can be transferred through a proper electrolyte in the form of O^{2-}, OH^-, or CO_3^{2-}. A fuel cell operated directly with solid carbon as the fuel is called as a direct carbon fuel cell (DCFC).[3,4] Normally, the activation energy of carbon is high so that high temperature is needed for the oxidation of carbon.[5] Therefore, fuel cells operated at high temperatures such as molten carbonate fuel cells (MCFCs), molten hydroxide fuel cells (MHFCs), and solid oxide fuel cells (SOFCs) are applied for electrochemically generating electricity from carbon. There

have been numerous investigations on DCFCs and several reviews have summarized them from different point of view.[6–10] Most studies have focused on DCFCs based on liquid electrolyte fuel cells such as MCFCs[11-13] and MHFCs[14–16]. There have been several investigations on applying carbon fuel in SOFCs but liquid metal or molten salt are added to the anode chamber for carbon delivering.[17-25] Liquid matter at high temperature is always a danger because it may cause leaking and corrosion. Therefore, SOFCs directly operated on carbon without liquid medium were proposed and investigated with Ar or CO_2 as carrying or gasifying gas.[26,27]

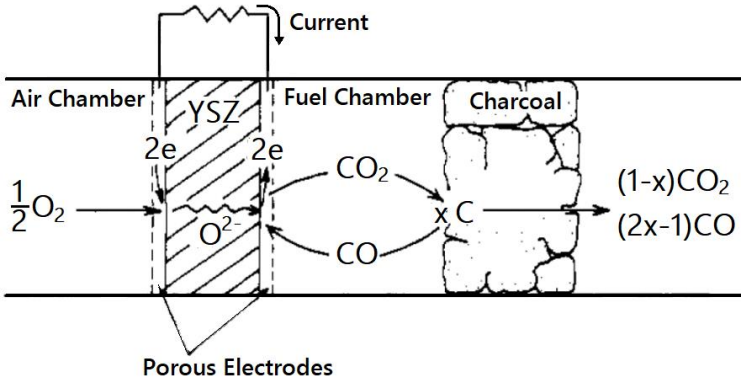

Fig.1 Schematic illustration of the operation mechanism of a direct carbon solid oxide fuel cell (DC-SOFC)[28]

Actually, carbon can be directly used as fuel of a SOFC without any liquid medium or purging gas, as illustrated in Fig.1. Nakagawa and Ishida[28] proposed the reaction mechanism of such a direct carbon solid oxide fuel cell (DC-SOFC) as that: Oxygen molecules in the air adsorb on the cathode, accepting electrons to become oxygen ions ($1/2\ O_2 + 2\ e^- = O^{2-}$). Then the oxygen ions go across through the electrolyte to the anode to oxidize CO, producing CO_2 and donating electrons

$$O^{2-} + CO = CO_2 + 2e^- \qquad (1)$$

The produced CO_2 molecules diffuse to the carbon fuel to perform the reverse Boudouard reaction, producing more CO

$$CO_2 + C = 2CO \quad (2)$$

Some of the CO molecules diffuse to the anode for the electrochemical oxidation reaction (1). The coupling of reactions (1) and (2) maintains a continuous generation of electricity from a DC-SOFC by consuming carbon fuel.

To verify the above mechanism of DC-SOFCs, Xie et al. [29] carried out an experiment to compare the performances of a DC-SOFC with a SOFC operated on pure CO. They obtained almost identical *I-V* curves and impedance spectra from the two kinds of cell, confirming that the anode reaction of a DC-SOFC is the electrochemical oxidation of CO. According to the mechanism, Tang et al.[30] applied Ag-GDC, which is a catalyst for the electrochemical oxidation of CO, as the anode material, and loaded Fe, which is a catalyst for the Boudouard reaction, on the carbon fuel. They obtained much higher performance from the DC-SOFC than that without any catalyst.

The feasibility of DC-SOFCs has been confirmed by continuous improvement of performance since the operation mechanism was first proposed in 1988, especially in recent years. Table 1 gives a brief review on the output performances of DC-SOFCs obtained in years. At the beginning, peak power outputs of only 6.5 and 68 mW were obtained at about 800 and 1000°C, respectively, on an YSZ electrolyte-supported SOFC fueled by charcoal.[28] With an effective area of 2 cm^2, these outputs corresponded to power densities of 3.3 and 34 mW cm^{-2}, respectively. The low performance can be attributed to the thick electrolyte (1.5 mm) and unoptimized electrode (porous

platinum). With the improvement of materials and fabrication techniques, an output power of 45 mW was obtained at 800°C from a tubular SOFC, with an electrolyte thickness of 0.3 mm and an effective area of 5.1 cm^2, operated on graphite powder in 2009.[31] Then a tubular Ni-based anode-supported ScSZ electrolyte SOFC, with an effective area of 10 cm^2, was operated on carbon black and an overall output power of 1040 mW was obtained at 850°C in 2010.[32] In the same year, a tubular DC-SOFC was successfully operated at a constant current of 30 mA for 37 hours.[33] Meanwhile, catalysts promoting the electrochemical oxidation of CO and the reverse Boudouard reaction were applied on the anode (Ag-GDC) and the carbon fuel (Fe), respectively, of a DC-SOFC and the output performance was enhanced by 7 times.[30] In 2011, a tubular anode-supported segmented-in-series 3-cell-stack, with an overall effective area of 5.1 cm^2, was operated with 5 wt.% Fe-loaded activated carbon,[34] and, an open circuit voltage of 3 V and an overall power output of 2400 mW were obtained at 850°C.[35] Later on, much effort has been devoted to investigation of DC-SOFCs on operating mechanisms[29,36,37], expanding carbon fuel sources (carbon from coal and biomasses) [38-44], optimizing materials[45-48] and improving configuration designs.[49,50] Recently, our group have developed a tubular electrolyte-supported segmented-in-series 3-cell-stack with carbon loaded outside the cell stack. This configuration enables more carbon integrated with the electricity generating system. The total effective area of the stack was 10.2 cm^2 (3.4 cm^2 for each unit cell). With 17 g carbon loaded, the DC-SOFC stack gave an OCV of 3.1 V and output power of 4100 mW at 800°C. It discharged at a constant current of 1 A for 19 h, revealing a discharging capacity of 19 Ah and an energy

capacity of 31.6 Wh.[51]

The superior discharging characteristics suggests that DC-SOFCs may be developed for portable application. Meanwhile, CO may be produced at a certain operating conditions. Therefore, DC-SOFCs may also be applied for gas-electricity cogeneration.[52] In this paper, we give a brief review on the oxidation of carbon through DC-SOFCs. First, we explain some basic principles of DC-SOFCs. Then we introduce applications, mainly on portable and gas-electricity cogeneration. Finally, some conclusions and perspectives are summarized.

Table 1. A brief history of output power and discharging characteristics of DC-SOFCs

Year	Configuration	Electrolyte (thickness)	Anode	Cathode	Fuel	Effective area (cm^2)	Operating temperature (°C)	Open circuit voltage (V)	Peak power (mW)	Discharging characteristics
1988[28]	Planar electrolyte-supported single cell	YSZ (1.5 mm)	Pt	Pt	Charcoal	2	802 1002	0.93 1.11	6.5 68	
2009[31]	Tubular electrolyte-supported single cell	YSZ (0.3 mm)	Ag	Ag	Graphite (0.8 g)	5.1	800	0.85	45	
2010[32]	Tubular anode-supported single cell	ScSZ	Ni-ScSZ/Ni-YSZ	LSM-ScSZ	Carbon black	10	850		1040	
2010[33]	Tubular electrolyte-supported single cell	YSZ	Ag	Ag	Activated carbon (0.6 g)	2.5	800	0.96	16	37 h at 30mA and ~0.5 V
2010[35]	Tubular electrolyte-supported single cell	YSZ	Ag-GDC (45:55)	Ag-GDC (45:55)	20 wt.% Fe-loaded activated carbon (0.54 g)	2.5	800	1.04	113	10 h at 70mA and ~0.7 V
2011[36]	Tubular anode-supported single cell	YSZ	Ni-YSZ	LSM-YSZ	5 wt.% Fe-loaded activated carbon (0.2 g)	2.3	850	1.10	975	
2011[37]	Tubular anode-supported segmented-in-series 3-cell-stack	YSZ	Ni-YSZ	LSM-YSZ	5 wt.% Fe-loaded activated carbon (1.2 g)	5.1	850	3.0	2400	1 h at 500 mA
2013[46]	Tubular electrolyte-supported single cell	4 wt.% Al_2O_3-doped YSZ	Ag-GDC (70:30)	LSM-YSZ (60:40)	5 wt.% Fe-loaded activated carbon (0.35 g)	1.2	850	1.11	302	4.3 h at 200 mA and ~0.7 V
2013[29]	Tubular porous YSZ - supported dense YSZ electrolyte single cell	YSZ (31 μm)	Infiltrated Cu-CeO_2	Ag	5 wt.% Fe-loaded activated carbon (0.16 g)	2	850	1.10	270	2 h at 200 mA
2014[45]	Tubular electrolyte-	LSGM	Ag-GDC	Ag-GDC	5 wt.% Fe-loaded	1.9	850	1.06	728	

	supported single cell	(0.15 mm)	(45:55)	(45:55)	activated carbon (0.17 g)		800	1.03	420	1.2 h at 400 mA
2015[52]	Electrolyte-supported single cell	1 wt.% Al_2O_3-doped-YSZ (0.16 mm)	Ag-GDC (70:30)	LSM-YSZ (60:40)	5 wt.% Fe-loaded activated carbon (1.0 g)	3.5	800	1.08	1120	3.3 h at 1000 mA 2.3 h at 1500 mA 1.5 h at 2000 mA
2015[52]	Electrolyte-supported segmented-in-series 2-cell-stack	1 wt.% Al_2O_3-doped-YSZ (0.16 mm)	Ag-GDC (70:30)	LSM-YSZ (60:40)	5 wt.% Fe-loaded activated carbon (1.4 g)	8.0	800	2.11	2552	1.1 h at 2000 mA
2016[47]	Anode-supported single cell	YSZ (27 μm)	$Ni_{0.9}Fe_{0.1}O_{\delta}$-YSZ	LSCF-GDC (70:30)	5 wt.% Fe-loaded activated carbon (2.5 g)	0.5	800	0.96	265	15 h at 50 mA and 0.85 V; 6 h at 100 mA and 0.75 V; 1.6 h at 200 mA and 0.65 V;
2017[51]	Electrolyte-supported segmented-in-series 3-cell-stack with carbon inside the cell stack	1 wt.% Al_2O_3-doped-YSZ (0.16 mm)	Ag-GDC (70:30)	Ag-GDC (70:30)	5 wt.% Fe-loaded activated carbon (3.0 g)	10.2	800	3.1	3200	3.5 h at 1000 mA 3.5 Ah 6.9 Wh
2017[51]	Electrolyte-supported segmented-in-series 3-cell-stack with carbon inside the cell stack	1 wt.% Al_2O_3-doped-YSZ (0.16 mm)	Ag-GDC (70:30)	Ag-GDC (70:30)	5 wt.% Fe-loaded activated carbon (17 g)	10.2	800	3.1	4100	19 h at 1000 mA 19 Ah 31.6 Wh

2. PRINCIPLES

2.1. Feasibility analysis of DC-SOFCs. The key point of that a DC-SOFC can work and give high performance is that CO is the favored product in the equilibrium gaseous composition of a C-O system with exceed carbon. Fig.2 shows the equilibrium gaseous composition of such a system with 1 mol of oxygen gas. We can see that at lower temperature, CO_2 dominates the composition while at high temperature, CO is the favored gas product. It can be seen from Fig.2 that when the operation temperature is 800°C, there are 1.6 mol of CO and 0.2 mol of CO_2, corresponding to a mol fraction of 89% and 11% for CO and CO_2, respectively, in the gaseous composition.

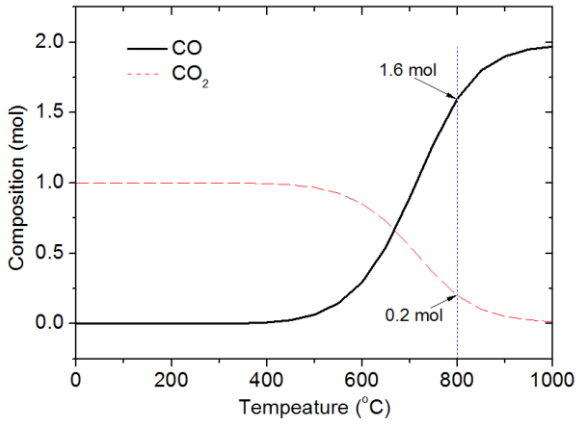

Fig.2 Equilibrium gaseous composition of a C-O system with 1 mol of oxygen gas and excess carbon

Note that in the anode chamber, the overall volume of the gases keeps increasing at atmospheric pressure once the operation of a DC-SOFC starts at a certain electrical current. This means the gases in the anode chamber tend to expand and expel out. Therefore there is little chance for the ambient air or oxygen coming into the chamber. This brings a superior feature for DC-SOFCs that they do not need strict sealing, resulting in easy assembling process and simple equipment.

2.2. Open circuit voltage. Considering the electrochemical reactions occurring at the cathode and anode, we see that the overall electrochemical reaction of a DC-SOFC is

$$1/2\ O_2 + CO = CO_2 \qquad (3)$$

The equilibrium gaseous composition can be used to calculate the open circuit voltage (OCV) of a DC-SOFC according to Nernst equation

$$E = E^0 + \frac{RT}{2F}\ln\frac{P_{CO}P_{O_2}^{1/2}}{P_{CO_2}} \qquad (4)$$

Where E^0 is the standard electro-motivated force (EMF), P_{O2} is the partial pressure of oxygen at the cathode, and P_{CO} and P_{CO2} are the partial pressures of CO and CO_2, respectively, at the anode. In most cases, the ambient air is taken as the oxidant for the cathode reaction, thus P_{O2} = 0.21. The calculated OCVs at different temperatures are shown in Fig.3 (dashed line).

However, the measured OCVs often do not fit exactly with the theoretical expectation. Sometimes they even exceeds the theoretical values. Tang et al.[30] measured OCVs of tubular DC-SOFCs with and without Fe catalyst, respectively. The results are shown in Fig.3. Compared to the theoretical calculation results, the OCVs for the DC-SOFC with Fe catalyst loaded on carbon fuel gives higher OCVs in the temperature range between 450 and 650°C. This can be explained as that, the reaction of a DC-SOFC is a kinetic process rather than a thermodynamic one. A complete equilibrium is impossible. According to the Nernst equation, the value of the OCV of a DC-SOFC is proportional to ln (P_{CO}/P_{CO2}). When the reaction rate of producing CO (mol s^{-1}) is faster than that of producing CO_2, as in the case of loading Fe catalyst on carbon, the instance value of OCV may be higher than that calculated from equilibrium assumption. This will result

in the OCV higher than the thermodynamic estimation. Xie et al. observed similar evidence in their experiments on measuring the OCVs of DC-SOFCs.[29]

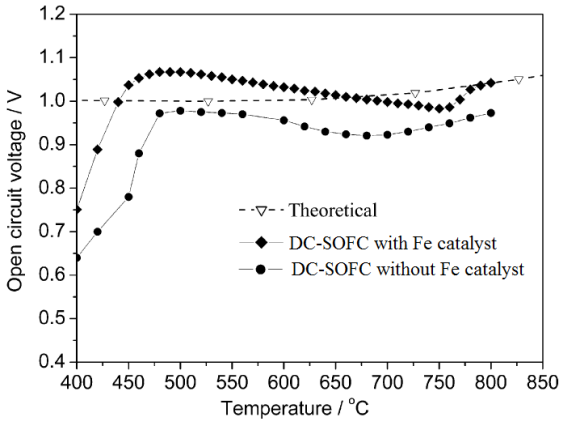

Fig.3 Open circuit voltages of DC-SOFCs obtained from experimental and theoretical calcultation[30]

2.3. Composition of emission. According to reactions (1) and (2) in the anode chamber of a DC-SOFC, one CO molecule reactant of (1) produces one CO_2. The CO_2 diffuses to the carbon to perform the reverse Boudouard reaction (2) to produce two CO molecules. One CO may diffuse back to the anode for the electrochemical oxidation reaction (1) and the other CO may emit out of the DC-SOFC. In this way, the operation of a DC-SOFC can be maintained and the only emitted gas is CO. However, the real situation is not that simple because not all the gaseous molecules in the anode chamber will participate the reaction (1) or (2), and the reaction rate of (1) may be quite different from that of (2). Cai et al. gave an initial analysis on the effect of relative reaction rate of (1) and (2) on the emission composition of a DC-SOFC.[35] Suppose the reaction rate of the electrochemical oxidation (1) is r_1 (mol s^{-1}) and of the reverse Boudouard reaction (2) is r_2 (mol s^{-1}). The rate r_1 can be manipulated by controlling the operating electrical current I (A)

$$r_1 = \frac{I}{2F} \qquad (5)$$

This is also the rate of consuming CO and producing CO_2 from reaction (1). In the reverse Boudouard reaction, CO_2 is consumed in a rate of r_2 and CO is produced in a rate of $2r_2$. Therefore, the overall CO producing rate of the DC-SOFC is

$$r_{CO}=2r_2-r_1 \qquad (6)$$

The overall CO_2 producing rate is

$$r_{CO2}=r_1-r_2 \qquad (7)$$

When r_1 is relatively slow and r_2 is fast, more CO is produced and the emitted gas composition contains more CO. In contrast, if r_1 is relatively high and r_2 is low, more CO_2 will emit from the DC-SOFC. Our experiments have shown good agreement with the above analysis.[36,52]

To enhance the electrical conversion efficiency, i.e., to generate more electricity from a certain amount of carbon, a relatively high r_1 and low r_2 should be applied. However, CO may be a more valuable product than electricity and more CO can be obtained by using a relatively quick r_2 and slow r_1. Different applications have different requirements and this will be discussed later in the following.

2.4. Effect of counter diffusion between CO and CO_2. In the coupling of reactions (1) and (2), (1) occurs at the anode but its reactant CO comes from reaction (2) which occurs at the carbon fuel; and the reactant CO_2 for (2) at carbon comes from (1) at the anode. Thus the distance between the carbon and the anode of a DC-SOFC, D_{ce}, may play an important role in affecting the counter diffusion between CO and CO_2, thus affecting the performance of the DC-SOFC. Xu et al.[37] developed a 2D numerical

model to describe the electrochemical/chemical reactions, ion/electron transport, mass transport and momentum transport in a tubular DC-SOFC. They conducted parametric simulations to evaluate the effects of distance between the carbon and the anode, D_{ce}, on DC-SOFC performance and found that the performance of DC-SOFC decreases with increasing D_{ce}. However, they also observed that the performance of DC-SOFC with large D_{ce} is still good enough, as shown in Fig.4, which indicates that the practical and large-scale DC-SOFC applications could be feasible. Our recent experimental results are well consistent with the simulation results.

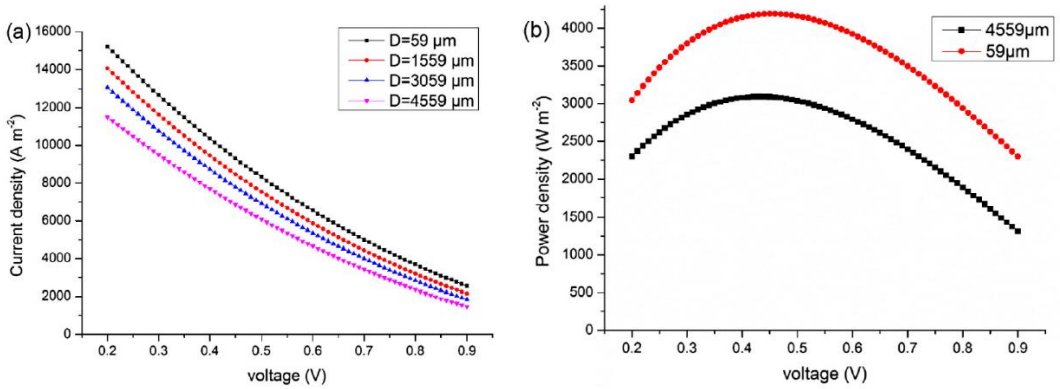

Fig.4 Effect of D_{ce} on (a) DC-SOFC output current density and (b) output power density at 1123 K.[37]

3. APPLICATIONS

As mentioned above, carbon can be oxidized through SOFCs at high temperature to generate electricity. Such a DC-SOFC is simple in equipment because it does not need any liquid medium or purging gas. The energy density of carbon is high. Theoretically, the charge capacity of carbon in a DC-SOFC could be as high as 8935 mAh g^{-1} which

is 24 times of that of graphite negative electrode in a lithium ion battery. Therefore, DC-SOFCs can be developed for portable applications. Meanwhile, pure CO which is more valuable than electricity can be effectively produced from a DC-SOFC operated at proper conditions. Thus, DC-SOFCs may also be developed for gas-electricity cogeneration applications.

3.1. DC-SOFCs for Portable Application. Currently, the most commonly used portable power sources are lithium ion and lead-acid batteries. Lithium ion battery has relatively high capacity but its security is still a problem. Lead-acid battery has the advantages of low cost and mature technology but its capacity is too low. Besides, they are rechargeable batteries or secondary batteries, meaning long time of charging which causes much inconvenience to customers. A portable DC-SOFC power source may overcome the issues of lithium ion and lead-acid batteries because it is safe with all-solid-state configuration and its capacity is high. More importantly, it generates electricity from carbon *in situ* and does not need long time charging. Seconds of replacing a cartridge of carbon powder may refresh a DC-SOFC power supply. To meet the terms conventional used in the area of portable power sources, a DC-SOFC for portable application is also called as a carbon-air battery.

Regarding the terms, DC-SOFC has several other names. We name it as direct carbon SOFC (DC-SOFC) because we have been working on SOFCs using a variety of fuels. Carbon is a novel solid fuel for SOFCs and it is directly placed in the anode chamber without any liquid medium or purging gas. For those who have been working on direct carbon fuel cells with different kinds of electrolyte, including molten carbonate, molten

hydroxide, and solid oxide, the DC-SOFC is named as solid oxide DCFC (SO-DCFC). For portable application, carbon can be taken as the active material of anode and the DC-SOFC can be viewed as a primary battery which is called as a carbon-air battery. Actually, there is no strict border between a fuel cell and a battery. An electrochemical cell for generating electricity is composed of cathode, electrolyte, and anode. Whether it is a battery or a fuel cell depends on the configuration of anode, as shown in Fig.5. A battery has its anode catalyst, current collector, and anode active material integrated (a). When the anode is divided into two parts, one part is the catalyst and current collector and the other part is the active material which is removable and replaceable, then the cell can be taken as either a battery or a fuel cell (b). For example, a zinc-air battery, with zinc as the active material, is also called as a fuel cell.[53] When the anode active material (generally a gas) is separated from the core cell and is supplied continuously from an external source, it is called a fuel cell (c). The DC-SOFC presented here belongs to the second situation (b), and the active anode material is solid carbon. In this aspect, it is called as a carbon-air battery or a carbon-air fuel cell. Although carbon is installed with the core cell (a SOFC), but can be removed, refilled, and replaced.

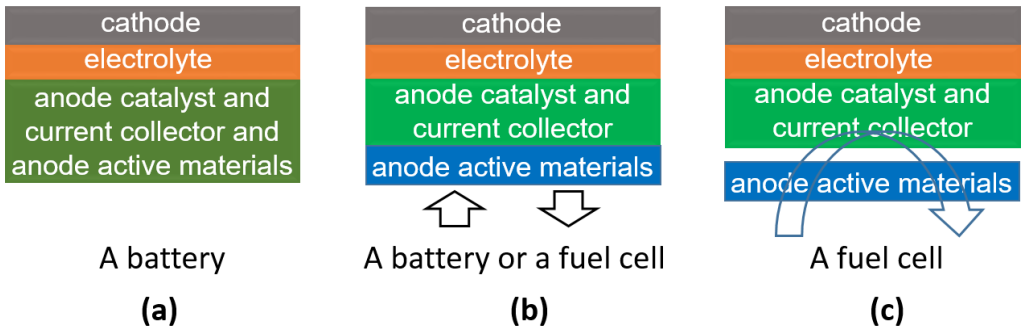

Fig.5 The difference between battery and fuel cell: (a) A battery; (b) A battery or a fuel cell; (c) A fuel cell

We have designed a portable power supply system based on a tubular segmented-in-series DC-SOFC, as shown in Fig.6.[49] A tubular segmented-in-series SOFC stack is located at the middle of the system, with the cathode inside and the anode outside. Surrounding the stack tube, there is carbon fuel in a heat conducting container. Some heating pipes are located around the container to provide the operating temperature. The system is wrapped by a heat insulator or heat exchangers to protect the heat from dissipation. A gas leading tube is set into the carbon fuel to lead out the producing gas, including CO, to a burner. The emitted CO is burned in the burner producing heat which is transferred to the heat exchangers to provide the heat needed for the reverse Boudouard reaction inside the container. Energy can be saved and the overall energy efficiency of the system can be improved in this way. Carbon fuel can be supplied or refilled through the inlet located on the up left corner. During the operation of this power source system, air is automatically fluxing through the inside of the tubular stack from the bottom to the upside.

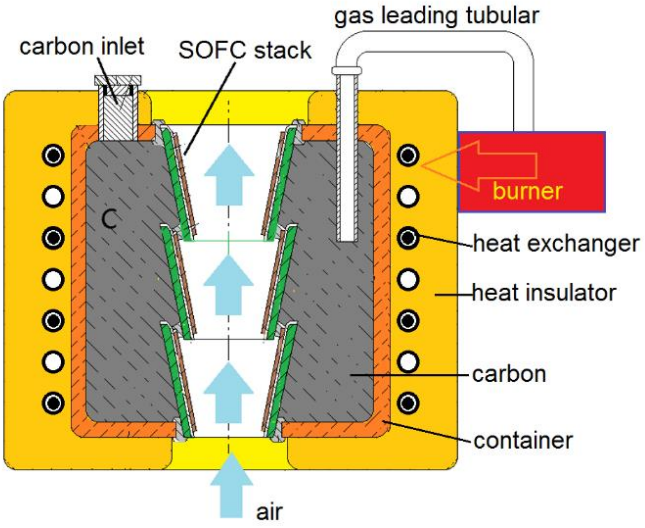

Fig.6 A designed portable power supply system based on DC-SOFC[49]

The tubular segmented-in-series SOFC stack can give a relatively high voltage with a small stack volume and this feature is especially suitable for portable application. Our group have devoted much effort on fabricating such kind of SOFC stack using slip casting[54.55], dip coating[56,57], and gel-casting[58] techniques. Bai et al. fabricated a tubular cone-shaped anode-supported segmented-in-series 11-cell-stack by dip-coating, as shown in Fig.7(a).[56] The total length of the stack was 9.5 cm and the diameter of the cone-shaped SOFC was 1.1 cm. The overall effective cathode area of the 11-cell-stack was 18.7 cm^2. The stack was operated with humidified methane (3% H_2O) as fuel and it provided a maximum power density of 421.4 mW cm^{-2}, corresponding to an overall output power of 8 W, at 800°C, as shown in Fig.7(b). The maximum volumetric power density of the stack was 0.9 W cm^{-3} at 800°C. Good stability was observed with 10 periods of thermal cycling test.

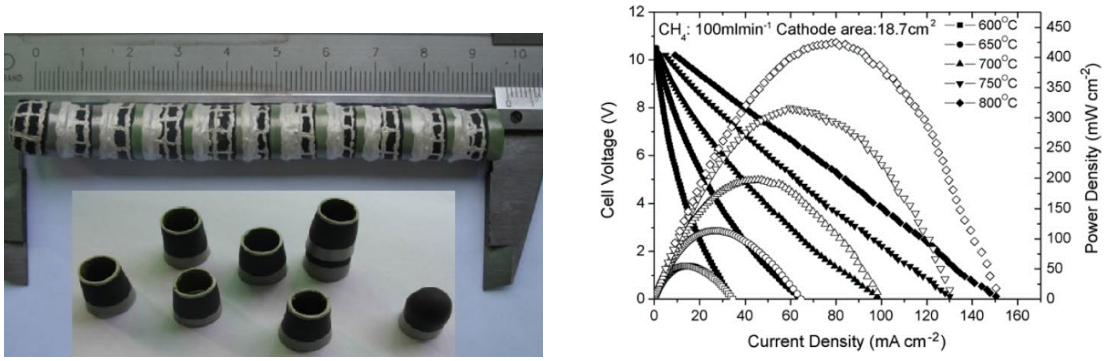

(a) (b)

Fig.7 A tubular cone-shaped anode-supported segmented-in-series 11-cell-stack (a) and the output performance of the stack operated on methane (b)[56]

Then, we operated the anode-supported cone-shaped single cells and a 3-cell-stack directly with 5 wt.% Fe loaded activated carbon as fuel, as illustrated in Fig.8.[35] 0.2 g

and 1.2 g of Fe-loaded carbon were filled in the each single cell and the 3-cell-stack, respectively. The effective area of the single cell was 2.3 cm^2 and the overall effective area of the 3-cell-stack was 5.2 cm^2.

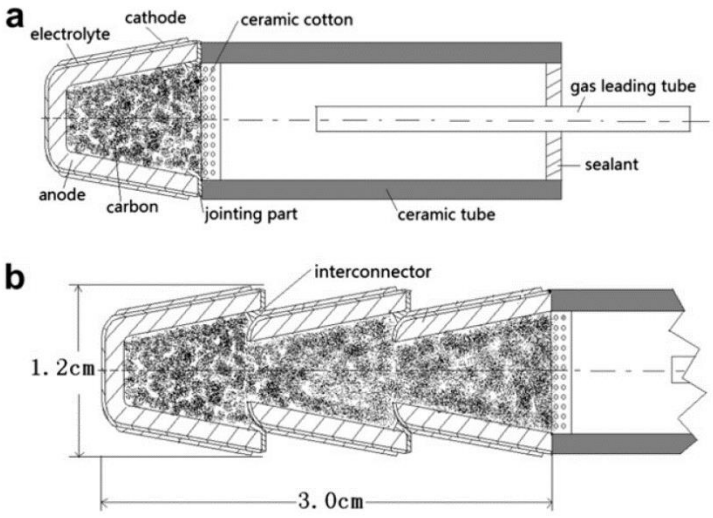

Fig.8 Schematic illustrations of a single DC-SOFC (a) and a 3-cell-stack (b)[34]

Fig.9 (a) shows a typical performance of the single cells at 850°C. The open circuit voltage is 1.1 V and the maximum power density is 424 mW cm^{-2} at 850°C. The result is four times of that reported by Wang et al. (104 mW cm^{-2} at 850 C).[32] Such improvement should be attributed to the function of the Boudouard reaction catalyst. Fig.9 (b) shows the discharging characteristics of the single cells operated at constant current of 0.5, 1.2, and 2.0 A (corresponding to current density of 0.22, 0.52 and 0.87 A cm^{-2}), respectively, at 850°C. Regardless of the initial performance of the cells, there appears a regularity that larger current results in shorter operating life. The cells operated at 0.5 A, 1.2 A, and 2 A give an operation life of about 60, 15, and 5 min, respectively. Chromatograph (GC) analysis shows that CO is the main exhausted gas in the initial stage of cell operating, which is consistent with the theoretical

thermodynamic equilibrium expectation.

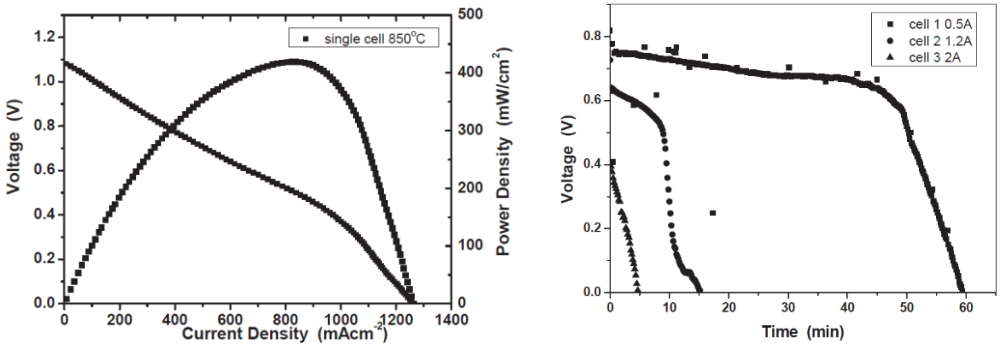

(a) (b)

Fig.9 Output performance of a single DC-SOFC (a) and discharging characteristics of a single DC-SOFC operated at different currents[35]

Fig.10 shows the output performance of the 3-cell-stack operated on 5 wt.% Fe-loaded activated carbon. The stack gives a maximum power of 2.4 W, corresponding to power density of 465 mW cm^{-2} (with a total active area of 5.2 cm^2), at 850°C. Taking the volume of the tubular stack, which is 3.4 cm^3 (with a diameter of 1.2 cm and length of 3.0 cm) as the bulk, we can see that the volumetric power density is 710 mW cm^{-3}. The output of this DC-SOFC stack is comparable to a SOFC stack, with the same configuration, operated on hydrogen.[56,57]

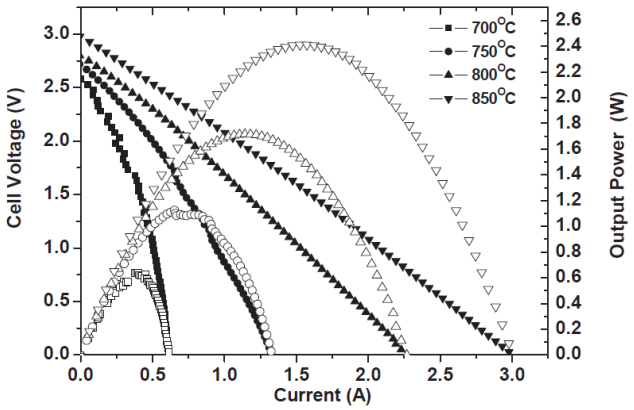

Fig.10 Output performance of 3-cell-stack of DC-SOFC[35]

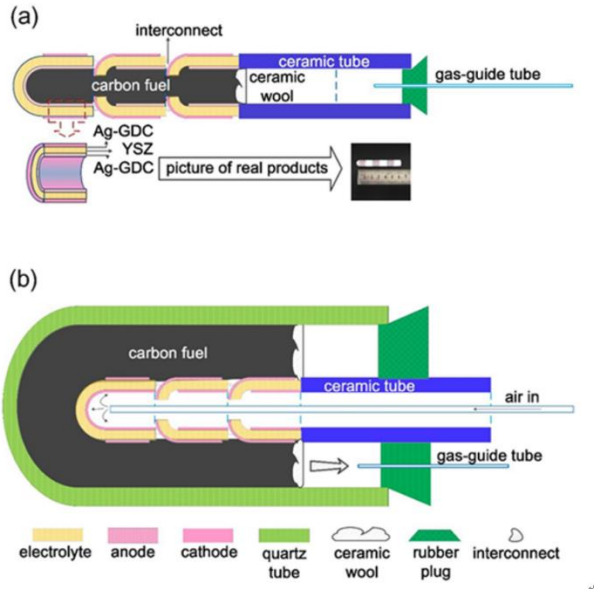

Fig.11 Schematic illustrations of 3-cell-stacks of DC-SOFC with carbon fuel loaded inside (a) and outside (b) of the tubular SOFC stacks[51]

Recently, we developed a tubular electrolyte-supported segmented-in-series DC-SOFC stack with carbon fuel loaded outside the stack tube, as illustrated in Fig.11.[51] Previously, we filled carbon fuel inside tubular cells or stacks as shown in Fig.11(a). The operating time (or discharging capacity) of such DC-SOFCs is not long enough because the amount of carbon filled is limited by the interior space of the cells or stacks. When carbon fuel is loaded outside the stack, as shown in Fig.11 (b), much more carbon fuel can be integrated with the stack. Actually, this configuration is more closed to the stack of the designed power source system as shown in Fig. 6. With an overall effective area of 10.4 cm^2 and 17 g carbon loaded outside, the stack gave an OCV of 3.1 V and an output power of 4100 mW at 800°C (Fig.12 (a)). It discharged at a constant current of 1 A for 19 h, as shown in Fig.12 (b). This corresponds to a discharging capacity of 19 Ah and an energy capacity of 31.6 Wh. As a comparison, the stack with 3 g carbon loaded inside discharged at 1 A for only 3.5 h, revealing a discharging capacity of 3.5

Ah and energy capacity of 6.9 Wh. For the DC-SOFC with carbon loaded outside the stack, the energy capacity of 31.6 Wh corresponds a mass energy density of 1.86 Wh g^{-1}. This value is significantly higher than the maximum energy density of current lithium ion batteries (~0.2 $W \cdot h \cdot g^{-1}$).

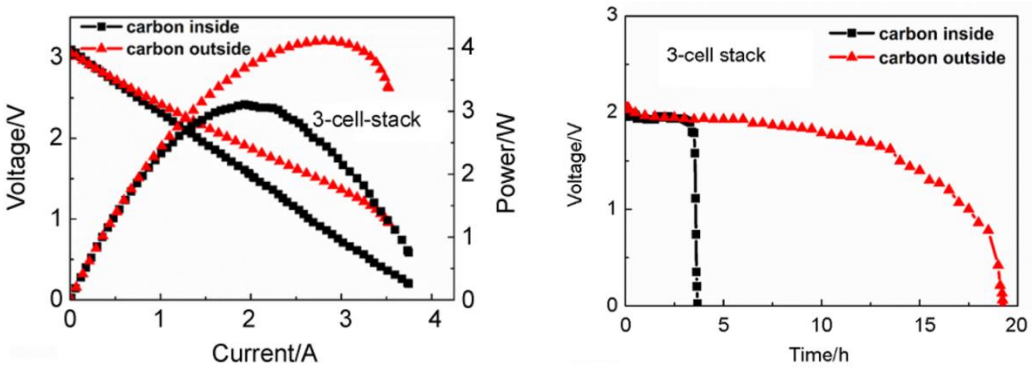

Fig.12 Output performances (a) and discharging characteristics (b) of 3-cell-stack of DC-SOFC with carbon inside and outside of the tubular SOFC stacks, respectively[51]

In contrast to lithium-ion batteries where graphite is the intercalation host, carbon is consumed in DC-SOFCs. Therefore, refueling capability of DC-SOFCs is important for practical applications. However, the DC-SOFC is far from mature compared to the lithium-ion battery. There are few data on the refueling capability of DC-SOFCs. Probably, the only report on refueling capability is from Xie et al.[59] After an initial operation and the carbon fuel was used up, they refueled the DC-SOFC and obtained completely identical performance as DC-SOFC was first operated.

3.2. Gas-electricity cogeneration. As mentioned above, the emissions of a DC-SOFC can be manipulated by controlling the relative reaction rates of the electrochemical oxidation of CO (1) and the reverse Boudouard reaction (2). A relatively larger rate of

the reverse Boudouard reaction leads to more CO production. According to Equations (6) and (7), when the oxidation rate of CO r_1 equals to the rate of the reverse Boudouard reaction r_2, there is no CO_2 emitted and the only product is CO. CO is an important chemical stock in chemical engineering industry. In most cases, CO is more valuable than electricity. Therefore, a DC-SOFC can also be used for gas-electricity cogeneration.[52]

When used for producing chemical products such as CO, a DC-SOFC can be viewed as a membrane reactor, as illustrated in Fig.13. The electrolyte is an oxygen permission membrane through which oxygen ions are provided for the electrochemical oxidation reaction. Active catalysts can be applied to the carbon fuel to speed the reverse Boudouard reaction for more CO production. Meanwhile, electricity is generated, mainly with an overall reaction of

$$C + 1/2\ O_2 = CO \qquad (8)$$

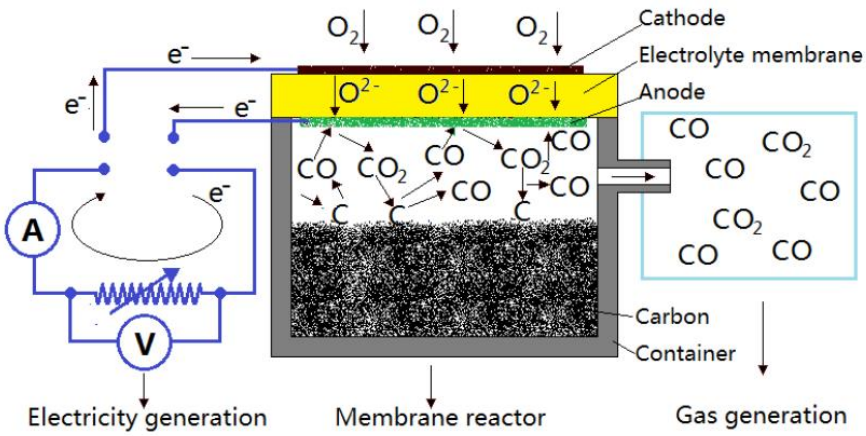

Fig.13 A membrane DC-SOFC reactor for gas-electricity cogeneration[52]

Xie et al. tested the gas-electricity cogeneration performances of single tubular DC-

SOFCs. The YSZ electrolyte-supported SOFCs for preparing the DC-SOFCs were with an effective area of 3.5 cm^2.[52] Each DC-SOFC was loaded with 1 g of 5 wt.% Fe-loaded activated carbon. Fig.14 shows the performances of typical SOFCs operated on hydrogen and carbon, respectively, at 800°C. As can be seen, the OCV of the DC-SOFC is 1.08 V and the peak power density is 320 mW cm^{-2}.

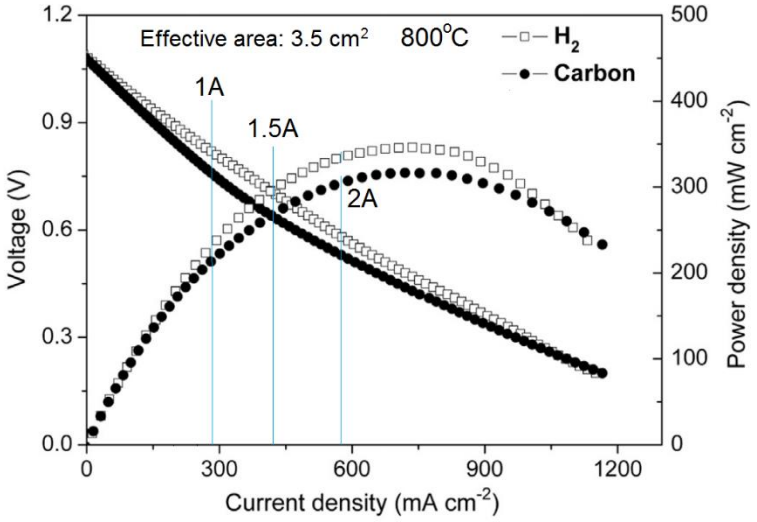

Fig.14 Performances of SOFCs operated on hydrogen and 5 wt.% activated carbon, respectively, at 800°C[52]

For the gas-electricity cogeneration tests, a flow meter and an online gas chromatography (GC) were sequentially attached to the outlet of a DC-SOFC to detect the flow rate and the composition of the produced gas. Three operating electrical currents, 1, 1.5, and 2 A (corresponding to current densities of 0.29, 0.43, and 0.57 A cm^{-2}, respectively) were selected for the investigation. Fig. 15 shows the electrical power output along with the rate of CO and CO_2 production for the cells operated at different currents. It can be seen that, both the power output and the CO production are decreasing while the CO_2 production is increasing with time. The CO decreasing is

caused by the consumption of carbon fuel (through the reverse Boudouard reaction) as the DC-SOFC is a fixed bed reactor with the solid carbon fuel positioned in the cell statically. With the carbon fuel being consumed, the active reaction sites are decreasing, resulting in a reduced rate of reaction (2). Meanwhile, according to Equation (5), the rate of reaction (1) does not change at a constant current. As a result, the rate of producing CO decreases while that of CO_2 increases with time because the rate of reaction (2), which produces CO and consumes CO_2, falls while the rate of reaction (1), which consumes CO and produces CO_2, keeps constant.

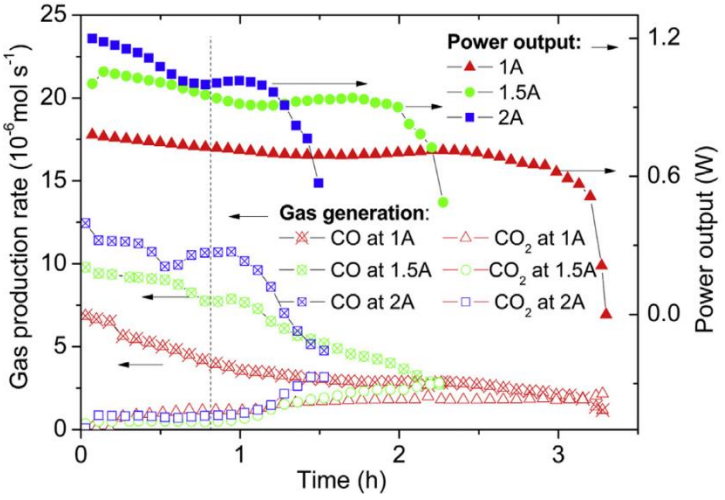

Fig.15 Gas producing rate and power output of the single DC-SOFCs operated at different currents, at 800°C[52]

As shown in Fig. 15, at the beginning of the cell operation, higher electrical current corresponds to higher electrical output power and higher CO production rate. The rate of reaction (2) decreases more rapidly at higher operating current because the carbon consumption (activity decreasing) is faster. Thus the cell has a shorter discharging time (smaller discharging capacity) due to insufficient CO for maintaining the cell operation

at a constant current. This fact is well consistent with our previous work.[30] Therefore, a high reaction rate is necessary for reaction (2) to obtain high electrical power and large amount of CO production.

When a DC-SOFC operates at a current I and voltage V, the electricity power produced is $P_e = IV$. Suppose it produces CO with rate of r_{CO}. The Gibbs free energy of the produced CO, which can be converted to electricity through reaction (1), is r_{CO} (G_{CO}-G_{CO2}), where G_{CO} and G_{CO2} are the molar Gibbs energy of CO and CO_2, respectively. The total output power is

$$P_o = P_e + r_{CO} (G_{CO}\text{-}G_{CO2}) \qquad (9)$$

The input power can be taken as the Gibbs energy change of complete oxidation of the consumed carbon

$$P_i = (r_{CO} + r_{CO2}) G_{CO2} \qquad (10)$$

The electrical conversion efficiency is $\eta_e = P_e/P_i$ and the overall conversion efficiency is $\eta_o = P_o/P_i$.

Fig. 16 shows η_e and η_o of the cells operated at different current at 800°C. Obviously, when the produced CO is considered as a kind of produced energy, the overall conversion efficiency is about twice of the electrical conversion efficiency. While the cell operated at higher current (and lower voltage) reveals lower electrical conversion efficiency, the overall conversion efficiency does not have a clear correlation with the operating current. This is consistent with the electrical conversion efficiency results shown in Fig. 9. When CO is considered in the overall conversion efficiency, the electrical conversion efficiency reduction caused by high current is compensated by the

increasing CO production.

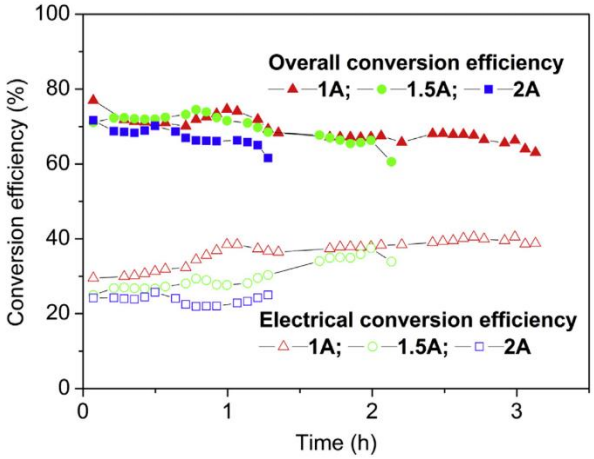

Fig.16 Electrical conversion efficiency, η_e, and overall conversion efficiency, η_o, of the DC-SOFCs operated with different current at 800°C[52]

Fig. 17 shows the power output and gas production of the two-cell-stack of DC-SOFC, operated at a current of 2 A (0.50 A cm^{-2}), at 800°C. We can see that just like the situation of the single cells, both of its power output and CO production decreases with time while CO_2 producing rate increases with time. The beginning power output of the stack is 2.5 W. The rate of producing CO is 27 ml min^{-1} (2.0×10^{-5} mol s^{-1}), and the rate of producing CO_2 is only 2.6 ml min^{-1} (1.6×10^{-6} mol s^{-1}). According to Equations (9) and (10), the overall output power and input power are 6.26 and 8.64 W, respectively. The electrical conversion efficiency is 28.9% and the overall conversion efficiency is 72.5%. When the cell is operated for 0.8 h, the electrical power drops to 2.1 W. The CO producing rate decreases to 8.9 ml min^{-1} (6.6×10^{-5} mol s^{-6}) and the CO_2 rate increases to 10.0 ml min^{-1} (7.4×10^{-6} mol s^{-1}), respectively. The overall output power is 3.37 W and the input power is 5.56 W. The electrical and overall conversion efficiencies are

38.1% and 60.6%, respectively.

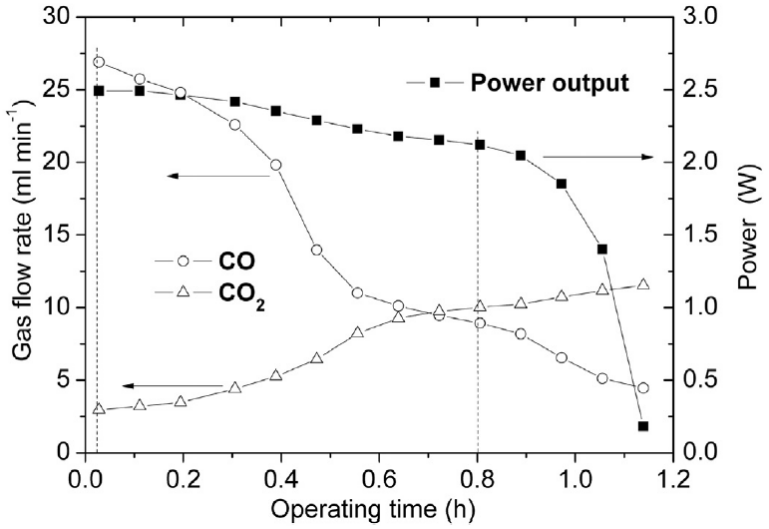

Fig.17 Gas-electricity cogeneration of a two-cell-stack of DC-SOFC operated at 2 A, at 800°C[52]

4. RESEARCH GAPS AND FUTURE PERSPECTIVES

Still, there are several challenges, such as heat management, removal of CO emission for portable application, continuous supply of carbon fuel, etc., for developing DC-SOFCs to practical applications.

4.1. Heat management. Suppose a DC-SOFC is equipped at a designed temperature of T_0. When it starts to operate at an electrical current of I, the temperature distribution will deviate from T_0 mainly because that the electrochemical oxidation of CO (1) occurring on the anode is an exothermic reaction while the reverse Boudouard reaction (2) is an endothermic one. Figure 18 is a schematic illustration of the temperature distribution in an operating DC-SOFC. The dashed line represents a theoretical temperature distribution while the solid line represents a simulated practical situation considering heat transformation.

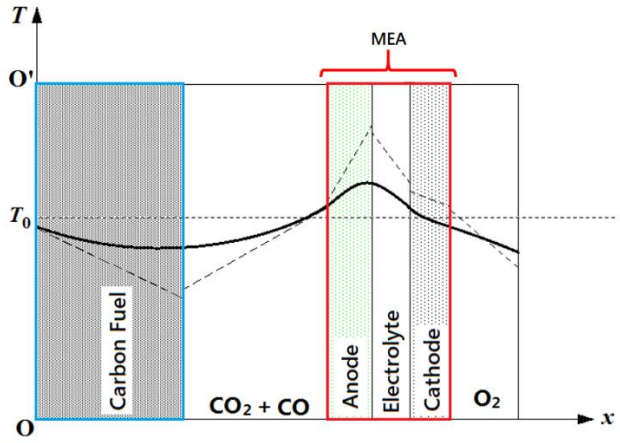

Fig.18 A schematic illustration of temperature distribution in an operating DC-SOFC

At 800°C and standard pressure, the enthalpy change ΔH and the Gibbs free energy change ΔG of reaction (1) are -282 kJ mol^{-1} and -189 kJ mol^{-1}, respectively, which means a heat of at least $-(\Delta H-\Delta G)$=93 kJ mol^{-1} is released through the electrochemical oxidation of CO. This heat increases the temperature of the anode, especially the anode-electrolyte interface (Fig.18), where the electrochemical oxidation of CO occurs at. Besides, for the anode, electrolyte, and cathode with a resistance of R_a, R_e, and R_c, respectively, a heat of I^2R_a, I^2R_e, and I^2R_c, will be produced from the corresponding element. Generally, the resistance of electrolyte dominates the overall resistance of the membrane electrode assembly (MEA) composed of the anode, electrolyte, and cathode. Consequently, the highest temperature is at the anode-electrolyte interface and the MEA is generating heat during the operation of the DC-SOFC.

Meanwhile, the enthalpy change of the reverse Boudouard reaction (2) is +170 kJ mol^{-1}, i.e., a heat of 170 kJ mol^{-1} is absorbed through the reaction, resulting in a temperature decrease of the carbon fuel. As mentioned above, the reactants of the reverse Boudouard reaction, CO_2 molecules, are produced from the anode. Therefore, more CO molecules

will perform the reaction at the location of carbon fuel closer to the anode. As a result, the lowest temperature is at the apparent surface of the carbon fuel. However, the heat from the MEA may be transferred to the carbon fuel through the convection of the CO-CO_2 gas and heat radiation between the anode and the carbon fuel, making the lowest temperature move to a depth from the surface of the carbon fuel.

The uneven distribution of temperature in a DC-SOFC severely affects its durability and efficiency. Over high temperature at the anode-electrolyte interface may cause rapid degradation of the anode and the electrolyte. In some cases, the MEA may be destroyed by some hot spots leading to a collapse of the overall DC-SOFC system. On the other hand, the reduced temperature at the carbon fuel may significantly retard the reaction rate of the reverse Boudouard reaction. An excess heat supply to the carbon fuel is necessary to maintain the reaction. If the heat is supplied from external of the DC-SOFC, then the energy efficiency is reduced. While, if the heat from the MEA can be transferred to the carbon fuel, not only the overheating of MEA can be moderated but also the energy efficiency can be elevated. To realize a uniform distribution of temperature, an enhanced heat transfer between different parts of a DC-SOFC is required.

4.2. Removal of CO from emission of DC-SOFC for portable application. In many cases, CO is emitted along with CO_2 from a DC-SOFC. For portable application, CO should be completely removed from the emission. This can be realized by catalytic combustion. Take the DC-SOFC power supply system shown in Fig.6 as an example, catalysts which promote the oxidation of CO can be applied in the burner. The heat

produced from the combustion can be transferred to the carbon fuel to maintain the temperature for the reverse Boudouard reaction. The most reported catalysts for oxidation of CO are noble metal-based, such as alumina-supported platinum-group metal catalysts,[60] zeolite supported platinum catalysts,[61] and metal oxide-supported gold catalysts.[62] $CuO\text{-}CeO_2$ mixed oxide catalysts have also been proposed as a promising candidate for removal of CO by oxidation.[63] However, most of these catalysts are investigated for removing CO from hydrogen fuel of proton exchange membrane fuel cells (PEMFCs). There have not been any reported experiments on the removal of CO from the emission of DC-SOFCs.

4.3. Continuous supply of carbon fuel. Most research work of DC-SOFCs has focused on fixed bed carbon supply, i.e., a limited amount of carbon fuel is statically placed in the DC-SOFCs. While carbon can be refilled through a designed inlet in the DC-SOFC system as shown in Fig.6, it is supplied in batches. A continuous supply of carbon fuel is necessary for large scale application, such as gas-electricity cogeneration, of DC-SOFCs. Although carbon powder or coal powder can be continuously blown into a SOFC with Ar or CO_2 as the carrying or gasifying gas,[8] the simplicity advantage of DC-SOFC is lost by gas feeding equipment. There has been rare work on continuous supply of carbon fuel to DC-SOFCs. Perhaps the only report is from Zhu et al.[38] They applied a U-shaped tube with open holes on the upper side as the delivering channel of carbon fuel (willow leaves), as shown in Fig.19. With this setting, a DC-SOFC has been operated at a constant current density of 150 mA cm^{-2} (~0.85 V) for 1000 minutes with a continuous supply of carbon-rich willow leaves through the U-shaped tube.

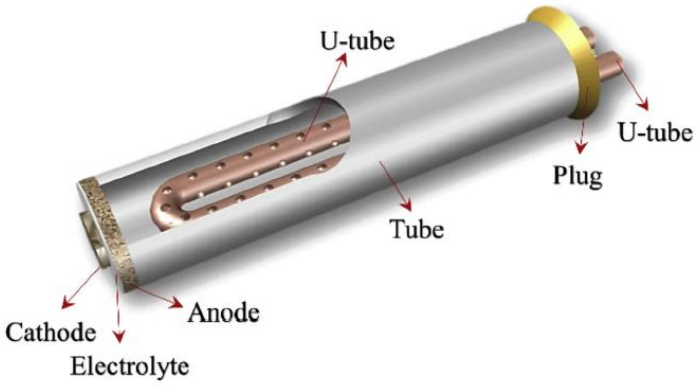

Fig. 19 A DC-SOFC with a U-shaped tube for continuous supply of carbon fuel[38]

5. CONCLUSIONS

Carbon can be electrochemically oxidized at high temperature to generate electricity and CO gas through a direct carbon solid oxide fuel cell (DC-SOFC), which is also named as solid oxide direct carbon fuel cell (SO-DCFC), carbon-air battery, and carbon-air fuel cell. The operating mechanism of DC-SOFCs is the coupling of electrochemical oxidation of CO at the anode and the reverse Boudouard reaction at the carbon fuel. Therefore, performances of a DC-SOFC can be significantly improved by applying proper catalyst (such as Ag-GDC) on the anode to promoting electrochemical oxidation of CO and loading catalyst (such as Fe) on carbon fuel to catalyze the reverse Boudouard reaction. The superior features of high power density, simple configuration, and good security make DC-SOFCs promising in portable applications. By manipulating the emission composition, DC-SOFCs can also be developed for gas-electricity cogeneration. To develop DC-SOFCs for practical applications, much work is necessary to resolve problems such as heat management, removal of CO from emission, and continuous supply of carbon.

■ AUTHOR INFORMATION

Corresponding author

*Email: jiangliu@scut.edu.cn

Notes

The authors declare no competing financial interest.

■ ACKNOWLEDGEMENTS

This work was supported by the National Science Foundation of China (NSFC, No. 91745203, 21276097), the Special Funds of Guangdong Province Public Research and Ability Construction (No. 2014A010106008), Guangdong Innovative and Entrepreneurial Research Team Program (No. 2014ZT05N200), and the NSFC-Guangdong Joint Fund (No. U1601207).

■ REFERENCES

(1) Minh, N. Q. *J. Am. Ceram. Soc*. **1993**, *76*, 563–588.

(2) Steele, B. C.; Heinzel, A. *Nature.* **2001**, *414*, 345-352.

(3) Dicks, A. L.; *J. Power Sources.* **2006**, *156*, 128-141.

(4) Carlson, E.J. EPRI report. Palo Alto: EPRI CA1013362, **2006**.

(5) Cao, D.; Sun, Y.; Wang, G. *J. Power Sources*. **2007,** *167,* 250–257.

(6) Rady, A. C.; Giddey, S.; Badwal, S. P.; Ladewig, B. P.; Bhattacharya, S. *Energy Fuels*. **2012**, *26*, 1471-1488.

(7) Giddey, S.; Badwal, S. P. S.; Kulkarni, A.; Munnings, C. *Prog. Energ. Combust.* **2012**, *38*, 360-399.

(8) Gür, T. M. *Chem. Rev.* **2013**, *113*, 6179-61206.

(9) Cao, T.; Huang, K.; Shi, Y.; Cai, N. *Energ. Environ. Sci.* **2017**, *10*, 460-490

(10) Zhong, Y.; Su, C.; Cai, R.; Tadé, M. O.; Shao, Z. *Energy Fuels*. **2016**, *30*, 1841−1848.

(11) Cooper J. F., Selman R. *ECS Transactions*. **2009**; *19*, 15-25.

(12) Jia, L.; Tian, Y.; Liu, Q.; Xia, C.; Yu, J.; Wang, Z.; Zhao, Y.; Li, Y. *J. Power Sources.* **2010**, *195*, 5581–5586.

(13) Elleuch, A.; Yu, J.; Boussetta, A.; Halouani, K.; Li, Y. *Int. J. Hydrogen Energ*. **2013**, *38*, 8514-8523.

(14) Kacprzak, A.; Kobylecki, R.; Bis, Z. *J. Power Sources.* **2013**, *239*, 409-414.

(15) Guo, L.; Calo, J.M.; Kearney, C.; Grimshaw, P. *Appl. Energ.* **2014**, *129*, 32-38.

(16) Zecevic, S.; Patton, EM.; Parhami, P. *Carbon.* **2004**, *42*, 1983-93.

(17) Nabae, Y.; Pointon, K. D.; Irvine, J. T. S. *Energ. Environ. Sci.* **2008**, *1*, 148-155.

(18) Jayakumar, A.; Küngas, R.; Roy, S.; Javadekar, A.; Buttrey, D. J.; Vohs, J. M. *Energ. Environ. Sci.* **2011**, *4*, 4133-4137.

(19) Xu, X.; Zhou, W.; Liang, F.; Zhu, Z. *Appl. Energ.* **2013**, *108*, 402-409.

(20) Hao, W.; He, X.; Mi, Y. *Appl. Energ.* **2014**, *135*, 174-181.

(21) Elleuch, A.; Halouani, K.; Li, Y. *J. Power Sources.* **2015**, *281*, 350-61.

(22) Yu, J.; Zhao, Y.; Li, Y. *J. Power Sources.* **2014**, *270*, 312-7.

(23) Jain, S. L.; Lakeman J. B.; Pointon, K. D.; Marshall, R.; Irvine, J. T. S. *Energ. Environ. Sci.* **2009**, *2*, 687-693.

(24) Jiang, C.; Ma, J.; Bonaccorso, A. D.; Irvine, J. T. S. *Energ. Environ. Sci.* **2012**, *5*, 6973-6980.

(25) Ahn, S. Y.; Eom, S. Y.; Rhie, Y. H.; Sung, Y. M.; Moon, C. E.; Choi, G. M. *Appl. Energ.* **2013**, *105*, 207-216.

(26) Li, S.; Lee, A. C.; Mitchell, R. E.; Gür, Turgut. M. *Solid State Ionics*. **2008**, *179*, 1549–1552.

(27) Wu, Y.; Su, C.; Zhang, C.; Ran, R.; Shao, Z. *Electrochem. Commun.* **2009**, *11*, 1265–1268.

(28) Nakagawa, N.; Ishida, M. *Ind. Eng. Chem. Res.* **1988**, *27*, 1181-1185.

(29) Xie, Y.; Tang, Y.; Liu J. *J. Solid State Electr.* 2013, 17, 121-127.

(30) Tang, Y.; Liu, *J. Int. J. Hydrogen Energ*. **2010**, *35*, 11188-11193.

(31) Tang, Y.; Liu, J.; Sui, J. *ECS Transactions*. **2009**, *25*, 1109-1114.

(32) Liu, R.; Zhao, C.; Li, J.; Zeng, F.; Wang, S. *J. Power Sources.* **2010**, *195*, 480-482.

(33) Tang, Y.; Liu, J. Phys-Chim. Sin. **2010**, *26*, 1191-1194.

(34) Tang, Y. Ph.D Thesis of South China University of Technology, 2011.

(35) Bai, Y.; Liu, Y.; Tang, Y.; Xie, Y.; Liu, J. *Int. J. Hydrogen Energ*. **2011**, *36*, 9189-9194.

(35) Cai, W.; Liu, J; Xie, Y.; Xiao, J.; Liu, M. *J. Solid State Electr.* **2016**, *20*, 2207-2216.

(37) Xu, H.; Chen, B.; Liu, J.; Ni, M. *Appl. Energ.* **2016**, *178*, 353–362.

(38) Zhu, X.; Li, Y.; Lü, Z. *Int. J. Hydrogen Energ*. **2016**, *41*, 5057-5062.

(39) Zhou, Q.; Cai, W.; Zhang, Y.; Liu, J.; Yuan, L.; Yu, F.; Wang, X.; Liu, M. *Biomass Bioenerg*. **2016**, *91*, 250-258.

(40) Cai, W.; Zhou, Q.; Xie, Y.; Liu, J.; Long, G.; Cheng, S.; Liu, M. *Appl. Energ*. **2016**, *179*, 1232-1241.

(41) Dudek, M.; Tomczyk, p.; Socha, R.; Hamaguchi, M. *Int. J. Hydrogen Energ.* **2014**, *39*, 12386-12394.

(42) Xu, K.; Chen, C.; Liu, H.; Tian, Y.; Li, X.; Yao, H. *Int. J. Hydrogen Energ*. **2014**, *39*, 17845-17851.

(43) Jiao, Y.; Tian, W.; Chen, H.; Shi, H.; Yang, B.; Li, C. *Appl. Energ*. **2015**, *141*, 200-208.

(44) Rady, A. C.; Giddey, S.; Kulkarni, A.; Badwal, S. P. S.; Bhattacharya, S.; Ladewig, B. P. *Appl. Energ*. **2014**, *120*, 56-64.

(45) Zhang, L.; Xiao, J.; Xie, Y.; Tang, Y.; Liu, J.; Liu M. J. Alloy Compd. **2014**, *608*, 272-7.

(46) Xie, Y.; Tang, Y.; Liu, J. *ECS Transactions* **2013**, *57*, 3039-3048.

(47) Yu, F.; Zhang, Y.; Yu, L.; Cai, W.; Yuan, Li.; Liu, J.; Liu, M. *Int. J. Hydrogen Energ*. **2016**, *41(21)*, 9048-9058.

(48) Xiao, J.; Han, D.; Yu, F.; Zhang, L.; Liu, J.; Zhan, Z.; Zhang, Y.; Dong, P. *J. Alloy Compd.* **2016,** *688,* 939-945.

(49) Liu J.; Liu, Y.; Tang, Y.; Bai, Y. A direct carbon solid oxide fuel cell power system. Chinese Patent CN102130354A, Jul 20, **2011**.

(50) Liu, J.; Zhang, L.; Liu, Y.; Yuan, L. A solid oxide fuel cell stack based on a single piece of electrolyte plate. Chinese Patent CN102130354A, Oct 8, **2014**.

(51) Wang, X.; Liu, J.; Xie, Y.; Cai, W.; Zhang, Y.; Zhou, Q.; Yu, F.; Liu, M. Acta. Phys-Chim.

Sin. **2017**, *33(8)*, 1614-1620.

(52) Xie, Y.; Cai, W.; Xiao, J.; Tang, Y.; Liu, J.; Liu, M. *J. Power Sources* **2015,** *277,* 1-8.

(53) Park, J.; Park, M.; Nam, G.; Lee, J. S.; Cho, J. *Adv. Mater.* **2015,** *27*, 1396-1401.

(54) Zhang, Y.; Liu, J.; Yin, J.; Yuan, W.; Sui, J. *Int. J. App. Ceram. Tech.* **2008,** *5*, 568-573.

(55) Ding, J.; Liu, J. *J. Power Sources* **2009,** *193*, 769-773.

(56) Bai, Y.; Wang, C.; Ding, J.; Jin, C.; Liu, J. *J. Power Sources* **2010,** *195*, 3882-3886.

(57) Bai, Y.; Liu, J. *Int. J. Hydrogen Energ.* **2009, 34**, 7311-7315.

(58) Liu, Y.; Tang, Y.; Ding, J.; Liu, J. *Int. J. Hydrogen Energ.* **2012,** *37*, 921-925.

(59) Xie, Y.; Wang X.; Liu, J.; Yu, C. *Acta Phys. -Chim. Sin.* **2017**, 33 (2), 386-392

(60) Manasilp, A.; Gulari, E. *Appl. Catal. B: Environ.* **2002,** *37*, 17-25.

(61) Igarashi, H.; Uchida, H.; Suzuki, M.; Sasaki, Y.; Watanabe, M. *Appl. Catal. A: Gen*. **1997**, *159(1),* 159-169.

(62) Schubert, M. M.; Plzak, V.; Garche, J.; Behm, R. J.; *Catal. Lett*. **2001,** *76(3-4)*, 143-150.

(63) Avgouropoulos, G.; Ioannides, T. *Appl. Catal. A: Gen.* **2003**, *244(1)*, 155-167.